Case Studies in Engineering Failure Analysis 4 (2015) 26–38

Contents lists available at ScienceDirect

Case Studies in Engineering Failure Analysis

journal homepage: www.elsevier.com/locate/csefa

Case study

A failure analysis study on the fractured connecting bolts of a filter press

Sh. Molaei [a,b], R. Alizadeh [c,*], M. Attarian [b,d], Y. Jaferian [b]

[a] Department of Materials Science and Engineering, School of Engineering, Shiraz University, Shiraz, Iran
[b] Department of Failure Analysis and Life Assessment, Razi Metallurgical Research Center, Tehran, Iran
[c] School of Metallurgical and Materials Engineering, University of Tehran, Tehran, Iran
[d] Department of Materials Science and Engineering, Sharif University of Technology, Tehran, Iran

ARTICLE INFO

Article history:
Received 30 March 2015
Received in revised form 13 July 2015
Accepted 22 July 2015
Available online 31 July 2015

Keywords:
Failure analysis
Fatigue failure
Filter press

ABSTRACT

The purpose of this study was to investigate the main causes of the co-fracture of sixteen connecting bolts of a filter press cylinder–piston system. Stress state of the bolts during the service conditions has been analyzed and the failure reasons were determined from the fractography analysis and gathered information. According to the obtained results, it was concluded that the bolts had failed by the fatigue mechanism. It seems that insufficient torque was used during assembly.

1. Introduction

Filter presses are utilized for solid–liquid separation by using an applied pressure which is usually generated by a hydraulic pump. Such filter presses have been employed in a variety of food industries. The present failed filter press machine was used in a cooking oil industry and consisted of four series of filter batches where each batch contained several filter plates. The load required to compress the filter plates was exerted by the main cylinder and piston hydraulic system. The hydraulic pump pressure was continuously monitored and recorded. This pressure increases in two steps to completely compress the filter plates; first from zero to 17 MPa and then from 17 MPa to 35 MPa, with sufficient holding times at each step. Finally, filter batches would be decompressed one by one to remove solid residues from the filter plates.

The proposed cylinder was jointed to the body of the press by sixteen M36 bolts of property Class 12.9. According to the customer's information, this filter press failed after being 50 months in service from the beginning. The failure was due to the co-fracture of 16 connecting bolts. Failed hydraulic system, including the main cylinder and piston and 16 fractured bolts are shown in Fig. 1 after accident. Also, the positions of the connecting bolts are shown in a white frame in Fig. 1a. According to the customer's information, fracture of the bolts and the accident were happened when the hydraulic pressure was in the highest level and filter plates were completely compressed. It has to be mentioned that all of the sixteen bolts were not accessible and two of them were not studied.

* Corresponding author. Tel.: +98 46831597; fax: +98 2146831570-7.
E-mail address: mrbalizadeh@ut.ac.ir (R. Alizadeh).

http://dx.doi.org/10.1016/j.csefa.2015.07.003

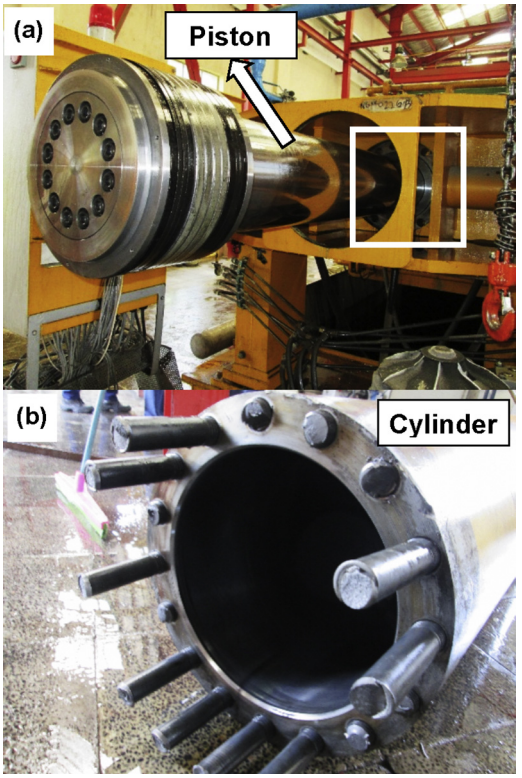

Fig. 1. The main piston and cylinder after accident: (a) the main piston together with the jointing position of the bolts, and (b) the cylinder with sixteen fractured bolts on it.

Several studies have been reported in the literature for the fracture of connecting bolts in different engineering systems [1–6]. For example, in one of these case studies [1], fracture of the worm gear connecting bolts was reported to be due to the two-way bending fatigue fracture. The main reason for the fracture was a large gap between the bolts and their matching internal gear bolt holes resulting from wear of the components. In another investigation [2], fatigue fracture of flange/housing assembly bolts of a gas compressor for polyethylene polymerization was studied and it was reported that increasing the bolt length for the same tightening torque tends to increase fatigue strength of the joint. However, there was no report on the failure analysis of similar filter press connecting bolts in the literature to the best of author's knowledge.

Accordingly, failure analysis of the broken connecting bolts was the main aim of the present paper to prevent similar failure accidents. SEM fractography and fracture mechanics were used for determining the main failure causes and mechanisms.

2. Methods of investigation

In order to evaluate the material composition and mechanical properties of the failed bolts, the mandatory tests of BS EN 898-1 (13) Class 12.9 standard were performed. For this purpose, the atomic absorption spectroscopy, Charpy impact, tensile, micro- and macro-hardness tests were done according to the ASTM E415 (14), ASTM E23 (12), ASTM A370 (12), and ASTM E384 (11) standards, respectively. Additionally, to study the microstructure of the bolts and carry out the decarburization test, some longitudinal sections were prepared for optical microscopic (OM) investigations. Also, the fracture surface of one of the failed bolts was studied by scanning electron microscope (SEM) after cleaning the fracture surface from the oil residues. Stress analysis was performed using both the fatigue calculations and linear theory of the bolted joints stiffness, to understand better the stress state of the bolts.

3. Results

3.1. Macrography and visual inspection

All of the fractured surfaces of the received samples were studied. Visual fracture studies of the bolts revealed that the fractures of nine of the bolts took place from the head zone, three of them from the thread region, two others from both

positions of the head and thread and the remaining two ones were not known. Here, it has to be mentioned that the bolts were produced by thread rolling process.

After some visual inspections, it was evident that most of the fractured bolts showed fatigue characteristics on their fracture surfaces. It is not a general rule, but the bolt which has the largest propagation surface is a strong candidate to be the first experienced the failure. Accordingly, and also for minimizing the costs, one of the bolts, with larger and more distinct fatigue fracture region, was chosen for further investigations (Fig. 2). This bolt can be considered as the probable first failed bolt in the system. It seems that the fatigue cracks were initiated from the thread root, and then propagated to the bolt center. Three typical morphological characteristics of fatigue fracture, including smooth fatigue region (light gray area), rough fatigue region (dark gray area), and overload region or final fracture (area with 45° slope) can be observed in the fracture surface of the proposed bolt. Also, it can be seen that about one–third of the fracture surface is belonged to the final fracture that occurred due to the overload. Schematic of the first fractured bolt with specific regions is also drawn in Fig. 2.

3.2. Material inspection

3.2.1. Chemical composition

Atomic absorption spectroscopy was used to determine the chemical composition of the bolt material (Table 1). The alloy composition satisfies the Class 12.9 standard, presented in Table 1.

3.2.2. Micro-hardness test

The Vickers micro-hardness tests were determined at points 1–3 (Fig. 3) according to the Class 12.9 standard to detect if the surface of the quenched and tempered bolts was decarburized. In addition, the micro-hardness tests were performed on the surface and center of the prepared sample. The micro-hardness test results are presented in Table 2. Based on the

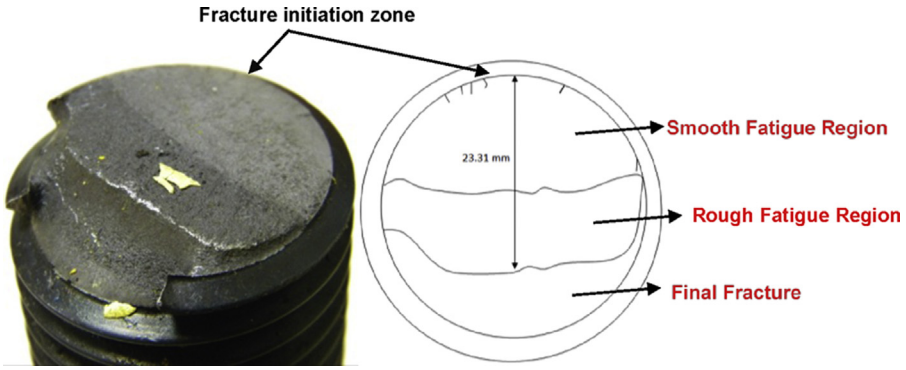

Fig. 2. Macrograph and schematic of fracture surface of one of the bolts.

Table 1
Material composition of the bolts together with the permissible values according to the Class 12.9 standard.

Steel of bolts	0.44	0.025	0.022	1.05	0.19 ± 0.01	<0.002
Class 12.9 standard	0.30–0.50	Max 0.025	Max 0.025	Min 0.30	Min 0.20	Max 0.003

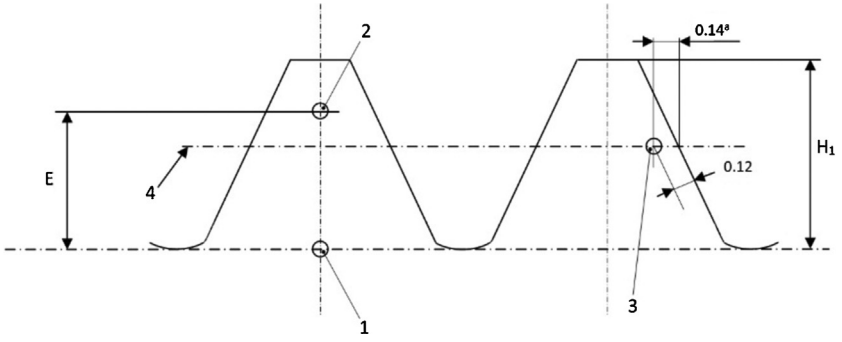

Fig. 3. Micro-hardness measurement points for detecting decarburization and carburization according to the Class 12.9 standard.

mentioned standard, the Vickers hardness at point 1 (HV point 1), minus 30 Vickers, shall be less than or equal to the Vickers hardness value at point 2 (HV point 2). Also, the Vickers hardness value at point 1 plus 30 Vickers shall be greater than or equal to the Vickers hardness value at point 3 (HV point 3). Moreover, the Vickers hardness of surface minus Vickers hardness of base should not exceed 30 Vickers (Eq. (1)). The permissible value of surface hardness for Class 12.9 is less than or equal to 435 HV 0.3. Therefore, it can be concluded that the micro-hardness test results satisfy the Class 12.9 standard and the no decarburization was detected on the surface of the bolt.

$$\begin{aligned} &\text{HV point2} \geq \text{HV point } 1 - 30 \\ &\text{HV point3} \leq \text{HV point } 1 + 30 \end{aligned} \tag{1}$$

$$\text{Surface Vickers hardness} - \text{Center Vickers hardness} \leq 30$$

3.2.3. Macro-hardness test

The Vickers macro-hardness test results are summarized in Table 3. As can be seen, the values of macro-hardness satisfy the Class 12.9 standard.

3.2.4. Tensile test

The tensile test results at room temperature are presented in Table 4. The permissible values of BS EN ISO 898-1 (13) for Class 12.9 mechanical properties are also included in this table. In this regard, the tensile test results are compatible with the Class 12.9 standard.

3.2.5. Impact test

Table 5 illustrates the results of Charpy V-notch impact tests at −20 °C. Regarding Class 12.9 standard, the value for the impact strength is under investigation and there is no report on the exact test data to be compared.

Table 2
Micro-hardness test results.

HV (300 grf)	Position
373	Surface
358	Center
381	Point 1
373	Point 2
381	Point 3

Table 3
Macro-hardness test results on the center of the bolt and the permissible values of the Class 12.9 standard.

387	HV (30 Kgf)
385–435 HV	Class 12.9 standard

Table 4
Room temperature tensile test results and permissible values of the Class 12.9 standard.

	R_m (MPa)	R_t (MPa)	$\%A$ $L_0 = 5.65\sqrt{S_0}$
Steel of bolts	1144	1315	12
Class 12.9 standard	Min 1100	Min 1220	Min 8

Table 5
Charpy impact test results at−20 °C.

Average (J)	Impact strength (J)	Dimension (mm × mm × mm)
23	22	55 × 10 × 10
	24	
	22	

3.3. Microstructural investigations by OM

Fig. 4a shows tempered martensite microstructure of the base metal at the center of the bolt. In order to examine decarburization on the surface of the quenched and tempered bolts, some metallography samples were prepared from threads and root sections. Fig. 4b and c shows the microstructures corresponding to the top and root of the thread, respectively. Subsequently, no decarburization was noticed on the surface of fasteners. As a result, the microstructure of the bolts satisfies the Class 12.9 standard.

3.4. SEM investigations

SEM micrographs of the sample are shown in Fig. 5. Fig. 5 shows that some heat treatment defects can be seen on the thread roots, which seem to be filled by some precipitates. Some fatigue cracks could be observed on the edge of the fractured surface (Fig. 6). The defects observed in Fig. 5 can be considered as fatigue nucleation sites whenever the applied stresses become greater than the fatigue limit of the material. It is also possible that more than one crack had been participated in the fatigue crack initiations. The SEM fatigue fracture surface image of the studied bolt, near to the nucleation point, is presented in Fig. 7. Some fatigue striations can be detected on the surface. Also, some secondary micro-cracks can be observed on the fatigue fracture surface [7].

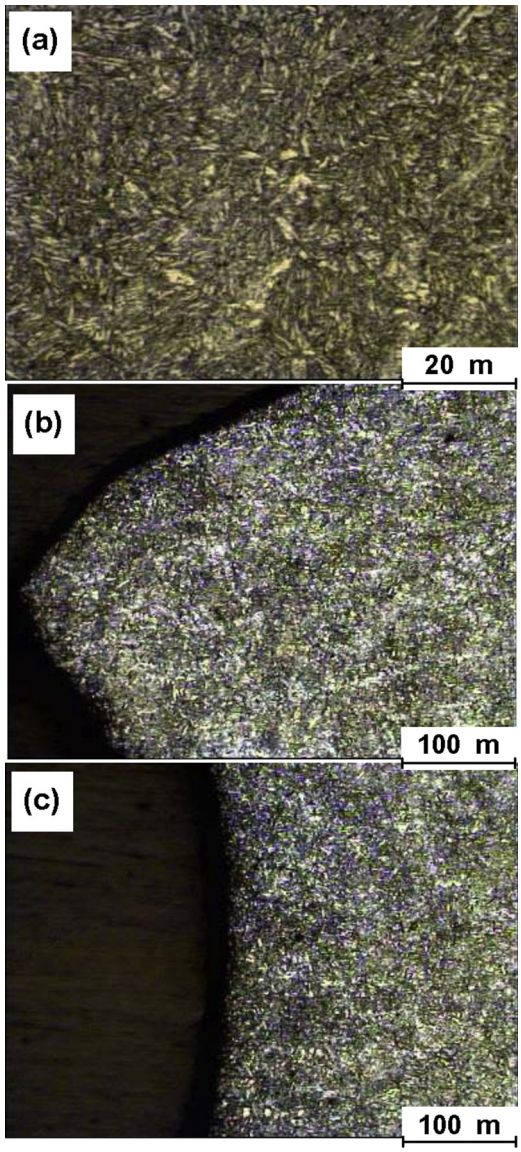

Fig. 4. Microstructure of the: (a) bolt center, (b) top, and (c) root of the thread.

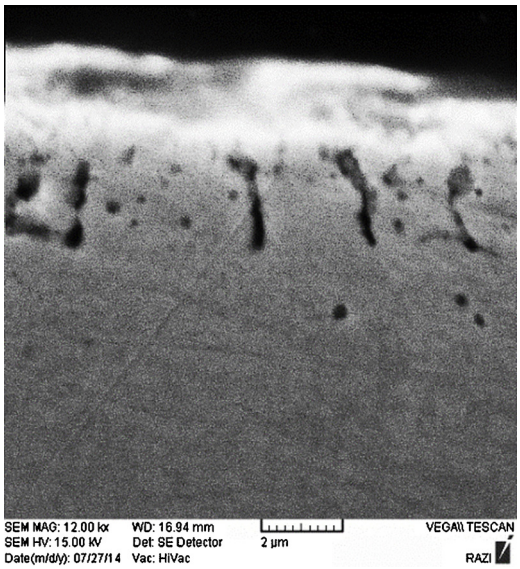

Fig. 5. Defects caused by heat treatment on the thread root.

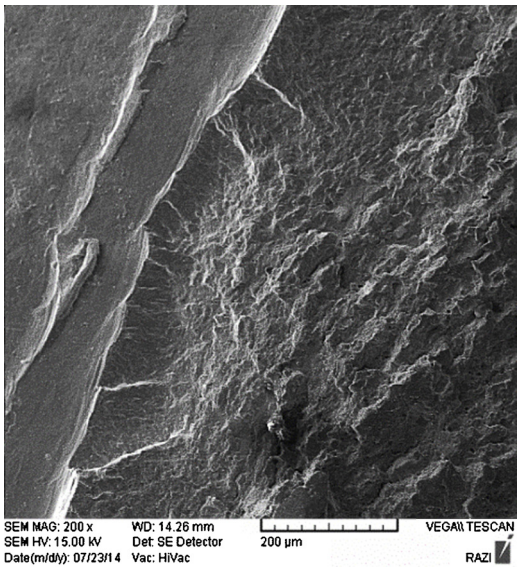

Fig. 6. SEM micrographs of the preliminary cracks on the fracture surface edge.

4. Stress analysis and discussion

4.1. Stress calculation by using fatigue striations and linear elastic fracture mechanics method

As indicated above, it seems that the type of the present fracture is fatigue fracture in nature. According to the BS 7910-06 standard, stress intensity factor range (ΔK) can be calculated from the crack growth rate (da/dN) by using Paris equation:

$$\frac{da}{dN} = A(\Delta K)^m \tag{2}$$

where A and m, materials constants of Paris equation. The da/dN values were calculated from the distances between the fatigue striations on the fracture surface by the use of SEM micrographs. For this purpose, after estimating the crack initial origin, the striation widths were calculated along two straight lines from the initiation zone to the final fracture [8–10]. By moving away from the origin, it was tried to find striations at different spacings from the initiation zone. In this regard, it has to be stated here that though each striation is produced by one stress cycle (and thus crack growth rate at that area can be

calculated simply by measuring the striation width, if the striation is chosen appropriately), not all stress cycles would produce a striation. This point is so important in all fatigue calculations, especially for the case of estimating total cycles experienced by the material in the second stage of fatigue from counting fatigue striations, since the overall crack growth rate might be smaller than the locally measured value from the striations.

After determining the crack growth rates at different crack lengths, the stress intensity factor range can be calculated from Eq. (2) by assuming $A = 1.35 \times 10^{-10}$ mm/cycle and $m = 2.25$ [11], respectively, or alternatively by using da/dN against ΔK curves, found in the literature for the same material. The calculated values of ΔK for different crack lengths (a) are listed in Table 6. The stress range ($\Delta\sigma$) can be calculated from ΔK values according to Eq. 3, where F is the shape factor. Assuming a crack initiated from the surface of the bolts (Fig. 8), and with considering tensile applied loads, the shape factor (F) for different crack lengths can be calculated from Eqs. (4)–(7) [12] as summarized in Table 7. In these equations, G is a

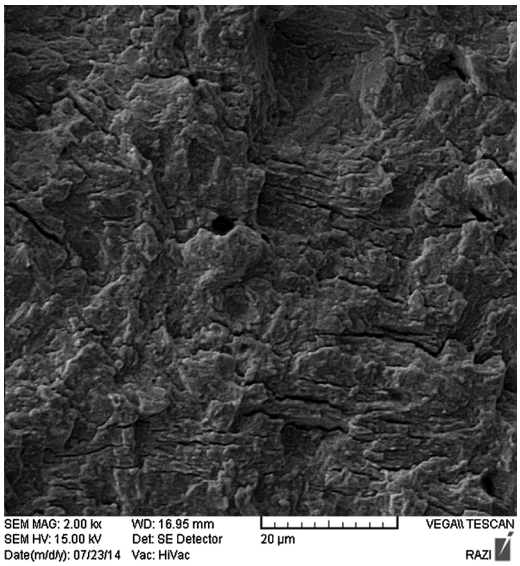

Fig. 7. Fatigue fracture surface of the bolt.

Table 6
Calculated ΔK values for different crack lengths.

Line	a (m)	da/dN (m/cycle)	ΔK (MPa$\sqrt{}$m)
1	0.00351	8.10×10^{-07}	47.8
1	0.00750	7.60×10^{-07}	46.4
1	0.00766	1.09×10^{-06}	54.4
2	0.00340	7.90×10^{-07}	47.2
2	0.00655	7.78×10^{-07}	46.9
2	0.00772	1.15×10^{-6}	55.8

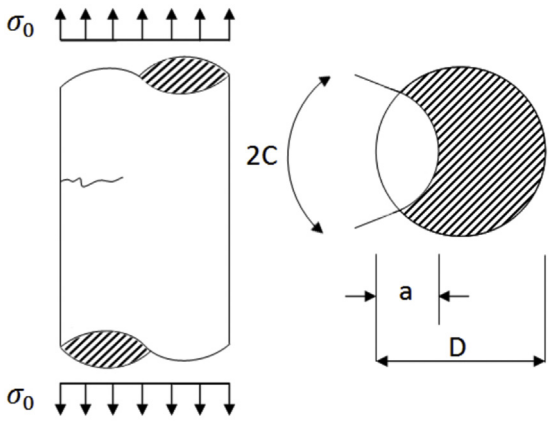

Fig. 8. Schematic of the crack propagation path in the bolts.

Table 7
Shape factor (F) and related parameters for different crack lengths.

D (mm)	a (mm)	B	Y	G	F
30	3.40	0.1779	0.8230	0.5986	0.7105
30.0	3.51	0.1837	0.8173	0.5994	0.7134
30.0	6.55	0.3428	0.6639	0.6348	0.8260
30.0	7.50	0.3925	0.6175	0.6513	0.8753
30.0	7.66	0.4009	0.6098	0.6544	0.8844
30.0	7.72	0.4040	0.6069	0.6556	0.8878

geometrical factor and Y has been defined for simplicity. Moreover, it should be noticed that because of the fracture location of the studied bolt, the diameter of suspected surface was considered to be equal to 30 mm.

$$\Delta K = F\Delta\sigma\sqrt{\pi a} \tag{3}$$

$$F = G[0.752 + 1.286\beta + 0.37Y^3] \tag{4}$$

$$G = 0.92\left(\frac{2}{\pi}\right)(\sec\beta)\left[\frac{\tan\beta}{\beta}\right]^{0.5} \tag{5}$$

$$Y = 1 - \sin\beta \tag{6}$$

$$\beta = \left(\frac{\pi}{2}\right)\left(\frac{a}{D}\right) \tag{7}$$

Calculated stress range ($\Delta\sigma$) values are summarized in Table 8. Hence, it seems that the stress ranges which have been experienced by the bolt are in the range of 397–643 MPa. Also, the alternative stress (σ_a) can be calculated from $\Delta\sigma$ values by using Eq. (8). Accordingly, it seems that the alternative stress which has been experienced by the bolt is in the range of 199–321 MPa. In this equation, the σ_{max} and σ_{min} are the maximum and minimum stresses experienced by the bolt, respectively.

$$\sigma_a = \frac{\sigma_{max} - \sigma_{min}}{2} \tag{8}$$

4.2. Stress calculation by using linear theory of the bolted joints stiffness

The linear theory considers a bolted joint as a set of springs which experience the same magnitude of elastic deformation when the bolt is tightened on the members. The linear theory is still accepted and included in most of the textbooks of mechanical engineering design [13–15]. A good reference about this issue is Williams et al. [16]. Fig. 9 illustrates the schematic of the joint between the cylinder and the body by using one of the bolts. When the load P is applied on the piston as a result of the force exerted by the hydraulic pump (when the filter plates are compressed), the maximum force on one of the bolts (P_{max}) can be considered in two states:

State *I* (If $F_i > (1 - C)P$): there would be no separation between the bolt and members, then: $P_{max} = F_i + CP$
State *II* (If $F_i < (1 - C)P$): there would be separation between the bolt and members, then: $P_{max} = F_i + P$

where F_i is the preload on the bolt, which is related to tightening torque (T) and bolt diameter (d) according to Eq. (9) [17,18], where p (thread pitch), μ (coefficient of friction between the male and female threads and the under head friction coefficient), d_2 (mean thread diameter) and d_u (under head mean diameter) have been considered as 0.18 and 4, 33.25 and 35.85 mm, respectively. Also, the C coefficient is called the stiffness ratio and can be calculated according to Eq. (10).

$$T = F_i[0.16p + 0.58\mu d_2 + 0.5\mu d_u] \tag{9}$$

Table 8
Calculated $\Delta\sigma$ values for different crack lengths.

Line	a (m)	$\Delta\sigma$ (MPa)
1	0.00351	637.8
1	0.00750	345.7
1	0.00766	396.6
2	0.00340	643.5
2	0.00655	396.1
2	0.00772	403.8

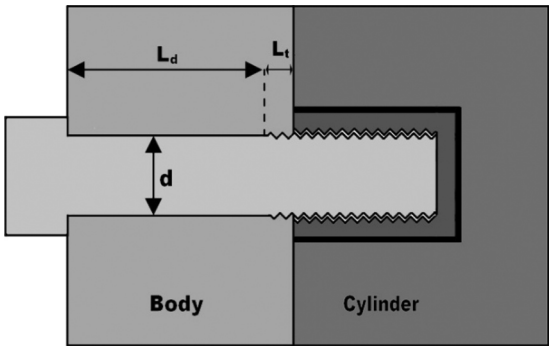

Fig. 9. Schematic of the bolt to display some parameters used in Eq. (13).

$$C = \frac{K_b}{K_b + K_m} \tag{10}$$

where K_b and K_m are bolt and member stiffness, respectively. K_b and K_m are defined as:

$$K_b = \frac{A_d A_t E}{A_d l_t + A_t l_d} \tag{11}$$

$$K_m = \frac{0.5774\pi E d}{2\ln\left(5\frac{0.5774l+0.5d}{0.5774l+2.5d}\right)} \tag{12}$$

$$L_G = l = l_b + l_t \tag{13}$$

where E, d, A_d, A_t, l_t, and l_d are Young's modulus (210 GPa), non-thread diameter, major diameter area of fastener, tensile stress area, length of threaded portion of grip, and length of unthreaded portion in grip, respectively (Fig. 9).

It has to be explained here that the elastic deflection of the bolt and members has to be the same when there is no separation (state *I*). As a result, some part of the applied load ($P_b = CP$) is carried by the bolt and the other part ($P_m = (1 - C)P$) would be carried by the members in this case. Variations of F_i and P_m with tightening torque are shown in Fig. 10, where the C coefficient was calculated to be about 0.195. It can be seen that F_i increases with tightening torque and at torques higher than a critical value, F_i would be higher than P_m and thus there would no separation (state *I*). However, applying lower tightening torques would result in a separation between the members and an increased imposed load on the bolt (state *II*).

Being in state *I* or *II* can greatly affect the alternative stress value. The alternative stress can be calculated from Eq. (8), where $\sigma_{max} = (F_i + CP)/A_t$ for state *I*, $\sigma_{max} = (F_i + P)/A_t$ for state *II* and $\sigma_{min} = F_i/A_t$ for both states. Consequently, the variation of the alternative stress with tightening torque is plotted in Fig. 11. An important point is that when there is no separation between the members (state *I*), the alternative stress was estimated to be about 27 MPa. However, when there is a separation between the bolts and members (state *II*), the situation is completely different and the alternative stresses (136 MPa) would be much higher than that obtained for state *I*. Here, it has to be mentioned that all of the presented data in Fig. 11a are obtained for $K_t = 1$. However, stress concentration factor would be certainly higher than 1 in real conditions, due to the stress

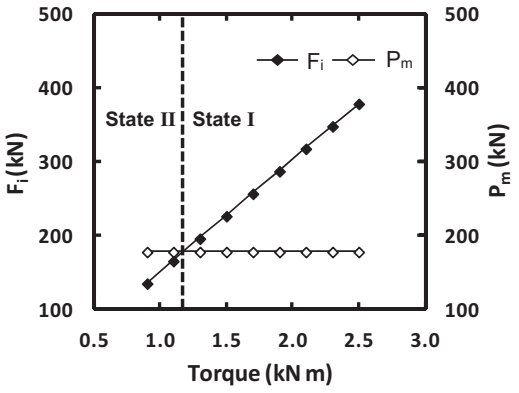

Fig. 10. The variations of F_i and P_m with tightening torque.

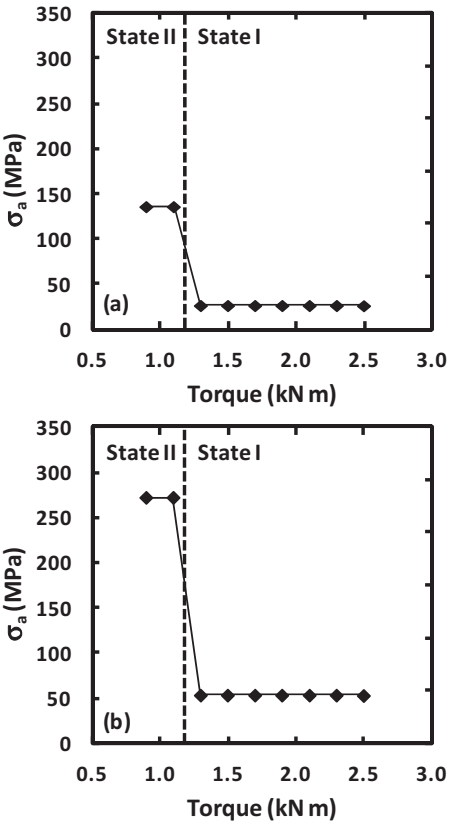

Fig. 11. The variation of σ_a with tightening torque for: (a) $K_t = 1$, and (b) $K_t = 2$.

concentration at thread roots and also for the fact that some part of the threads are out of the body (Fig. 1b). Maximum stress concentration would vary along the bolt length and it was shown that it can be in the range of 1.5–5 [19]. In the present case, a $K_t = 2$ has been assumed to show the minimum effects of stress concentration. However, it should be noticed that the actual stress concentration factor can be even much higher than this value. Calculated values of alternative stress, by assuming $K_t = 2$, are shown in Fig. 11b. In these conditions, the alternative stress was estimated to be 53 and 272 MPa for the states *I* and *II*, respectively. Thus, it can be observed that being in state *I* or *II* can greatly affect the alternative stress and σ_a becomes much higher than the fatigue limit of the material (190 MPa [20]) in state *II*.

Obtained $\sigma_a = 272$ MPa for state II is in well agreement with the alternative stress range which was calculated by using the fatigue striations in part 4.1 ($\sigma_a = 199$–321 MPa). This fact confirms well the occurrence of separation between members during the service life (state *II*) and also the presence of stress concentration. If there was no separation, the alternative stress could not reach to such high levels and result in fatigue of the bolts.

In addition to the alternative stress, two other important design parameters, the static safety factor (n) and fatigue safety factor (n_f), would also be affected greatly by the tightening torque. These parameters can be calculated from Eqs. (14) [13] and (15) [21], respectively.

$$n = \frac{S_p A_t - F_i}{CP} \tag{14}$$

$$\frac{\sigma_a}{S_e} + \frac{\sigma_m}{S_{ut}} = \frac{1}{n_f} \rightarrow n_f = \frac{S_e S_{ut}}{\sigma_a S_{ut} + \sigma_m S_e} \tag{15}$$

where S_p,σ_m, S_{ut}, and S_e are the proof stress (1144 MPa), mean stress, ultimate tensile stress (1315 MPa) and endurance limit (190 MPa), respectively.

Calculated n and n_f values are shown in Fig. 12a, by considering $T = 1.1$–2.5 kN m and $K_t = 1$. It can be observed that the n values would simply decrease with increasing tightening torque. However, the situation is more complicated for n_f, where there is an optimum torque value at which the fatigue safety factor is maximum. Therefore, increasing or decreasing the tightening torque is not beneficial always and an optimum value of torque should be considered for each case.

By comparing both the static and fatigue safety factors, it is clear that non real safety factors would be obtained by considering only the static conditions without considering the fatigue important role. For example, it can be observed that at

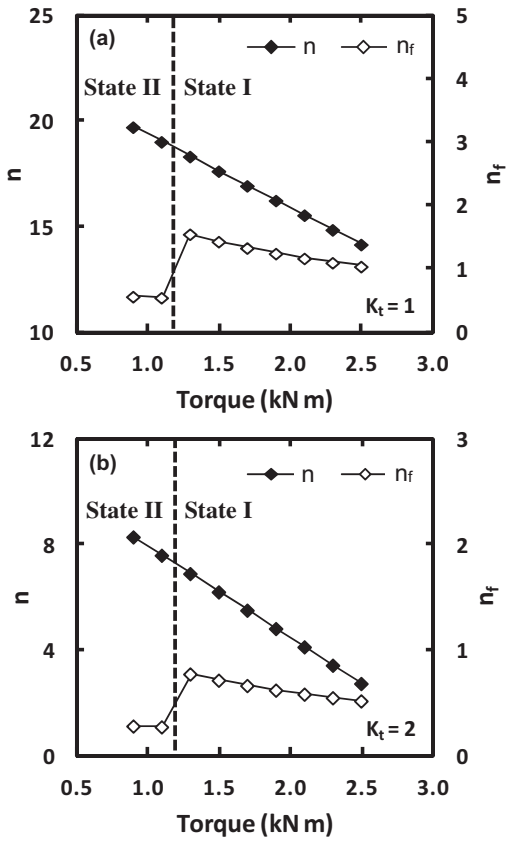

Fig. 12. The variations of n and n_f with tightening torque for: (a) $K_t = 1$, and (b) $K_t = 2$.

$T = 2.0$ kN m, $n \sim 15$ and $n_f \sim 1$ would be obtained which shows significance of fatigue calculations in real safety factor determination. It has to be mentioned that all of the presented data in Fig. 12a are obtained for $K_t = 1$. Calculated values of n and n_f for $K_t = 2$ are shown in Fig. 12b. Obtained results show that with assuming $K_t = 2$, the value of n_f would be less than 1 for all torque values. As a result, probability of fatigue occurring would be so high in real service conditions. Since $T = 2.0$ kN m was used for tightening of the bolts in service, as claimed by the customer, n and n_f of about 4 and 0.5 would be calculated for this condition, respectively. Thus, it seems that the claimed safety factor of 4 by the customer was obtained for just static loading.

To have a better representation of the data, Goodman diagram together with the present data points are shown in Fig. 13. Also, it was suggested to use modified Goodman diagram whenever some stress concentration exist in real working

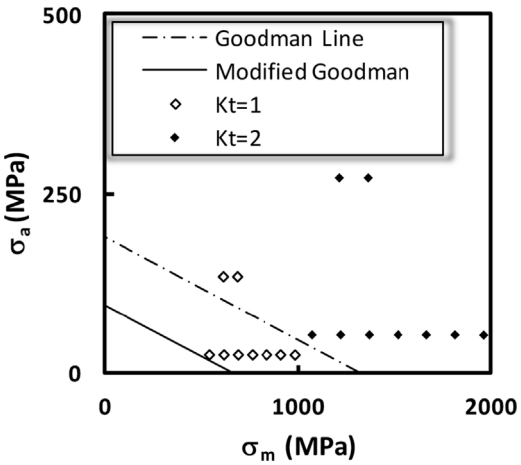

Fig. 13. Goodman modified diagram and the present data for different stress concentration factors.

conditions [22]. As can be seen in this figure, by increasing K_t from 1 to 2, the Goodman line and data points shift to lower and higher values, respectively. By assuming $K_t = 1$, some of the data points, which are belonged to state *I*, fall below the Goodman line (safe region) and only some pints (belonging to state *II*) fall above the line. However, in the case of $K_t = 2$, all of the data points, both from the states I and II, fall above the Goodman modified line, indicating that the conditions is suitable for fatigue of the bolts.

4.3. Failure causes

According to the stress calculations in previous sections, it seems that the cyclic stresses were designed to be lower than the fatigue limit of the bolt steel. However, if there was a separation between the members because of the low tightening torques, the cyclic stresses could be higher than the fatigue limit. In this manner, fatigue cracks would propagate through the thickness with each cyclic stress. Also, in addition to the role of tightening torques in increasing the real cyclic stresses, surface defects can play an important role in promoting fatigue in the proposed bolts. Since most of the fatigue cracks have been nucleated at the surface, surface and manufacturing effects seem extremely important. The small surface defects can fascinate the crack initiation. Hence, after initiation of fatigue cracks as the result of the increases stress, the cracks would continue to growth and the cross section area would be lower and lower and the stresses experienced by the remained area would be higher and higher with further propagation of the fatigue cracks toward the center of the bolts. In this condition, the crack length reaches to a critical value where, the stresses on the remained area exceed the fracture stress of the material and thus, final catastrophic fracture occurs.

In the present failure case, it seems that fatigue fracture has initiated from one of the thread roots (where stress concentration is high). Also, surface defects like those produced by heat treatment or machining, can act as fatigue crack nucleation sites and since, whenever the stresses were high enough, propagation of cracks could occur. Fatigue crack has initiated and propagated in all bolts, since fatigue characteristic were evident on the fracture surfaces of all studied bolts.

By assuming the fact that the bolts were tightened with $T = 2.0$ kN m, the static safety factor would be obtained to be about 4. However, considering only the static loading condition is so away from the real conditions and can result in catastrophic failures. As explained in the stress calculation part, the fatigue safety factor would be less than 1 even with considering a tightening torque of 2.0 kN m, where there would be no separation between the bolts and members. The situation would be even worse when smaller torques were used for tightening and the fatigue safety factor would be even smaller in this condition. On the other hand, there would be increased wear in the case of small tightening torques, which can promote fatigue initiation. Accordingly, it can be concluded that week tightening of some of the bolts can increase the cyclic stresses on bolts and severity of the fatigue damage. Service life of the bolts showed that the occurred fatigue damage was low cycle in nature and the cyclic stresses were probably a small away from the safe region.

After discussing the effects of different parameters on the promotion of fatigue in the present failure case, it is important to prevent future failures by appropriate precautions about these factors. One of the most important points which should be controlled periodically is the tightening torques on the bolts, which should be in the safe range to prevent separation between members. Another important job is to use thread rolled bolts instead of machined ones, to have a better surface quality in the thread roots, with less surface defects. Additionally, the surface quality should be examined after any heat treatments. An important point which has to be mentioned is that there should be an instruction for periodic check of the bolts by NDT methods at specific life time intervals (defined and provided by the designer), to prevent similar failures in future. In addition to the NDT methods, paying attention to the noise produced by the machine would be so helpful in determining possible separation between members, since there would be unusual noises if the tightening torques were lower than that required for preventing separation. Finally, true and on–time exchange of the parts which may show finished life, can prevent huge failures in future.

5. Conclusion

Failure causes of the co-fracture of sixteen connecting bolts of a filter press were investigated. Fracture surfaces of the bolts showed distinct fatigue characteristics and thus the fracture cause was determined to be progressive growth of the fatigue cracks. It was shown that, probably low tightening torques were used for the assembly. Accordingly, the bolts failed due to the separation between members and thus the increased alternative stress on the bolts to beyond the fatigue limit of the material, which favors the conditions for failure by the fatigue mechanism. Also, stress concentration at the bolt roots and surface defects seem to be important parameters in promotion of crack initiation.

Acknowledgment

Authors should say their thanks to Mr. Razeghi from the Razi Metallurgical Research Center for his helps.

References

[1] Li L, Wang R. Failure analysis on fracture of worm gear Connecting Bolts. Eng Fail Anal 2014;36:439–46.

[2] Griza S, da Silva M, dos Santos SV, Pizzio E, Strohaecker TR. The effect of bolt length in the fatigue strength of M24x3 bolt studs. Eng Fail Anal 2013;34:397–406.
[3] Krishnaraj N, Bala Srinivasan P, Muthupandi V. Investigation of a mounting bolt failure in an automobile air brake assembly. Pract Fail Anal 2003;3:69–72.
[4] Reitz W. Failure of bolt threads exposed to shear stress. J Fail Anal Prevent 2013;13:551–4.
[5] Curtis LR. Metallurgical failure analysis of fasteners in an impeller assembly. J Fail Anal Prevent 2006;6:17–22.
[6] Mohammadi M, Reza Salimi H. Failure analysis of a gas turbine marriage bolt. J Fail Anal Prevent 2007;7:81–6.
[7] Henry G, Horstmann D. DE FERRI METALLOGRAPHIA: Fractography and Microfractography, vol. 5. 1979;p. 282.
[8] Hershko E, Mandelker N, Gheorghiu G, Sheinkopf H, Cohen I, Levy O. Assessment of fatigue striation counting accuracy using high resolution scanning electron microscope. Eng Fail Anal 2008;15:20–7.
[9] Connors WC. fatigue striation spacing analysis. Mater Charact 1994;33:245–53.
[10] DeVries PH, Ruth KT, Dennies DP. Counting on fatigue: striations and their measure. J Fail Anal Prevent 2010;10:120–37.
[11] Barsom JM. Fatigue-crack propagation in steels of various yield strengths. Trans ASME J Eng Ind 1971;4:1190.
[12] Forman RG, Shivakumar V. Growth behavior of surface cracks in the circumferential plane of solid and hollow cylinders. Fract Mech 1986;17:59–74 (ASTM 905).
[13] Shigley JE, Mischke CR. Mechanical engineering design. 6th ed. McGraw Hill; 2001.
[14] Bickford JH. The Handbook of bolts and bolted joints. Hardback edition, Dekker; 1998.
[15] Norton NR. Machine design: an integrated approach. 2nd ed. Prentice Hall; 2000.
[16] Williams JG, Anley RE, Nash DH, Gray TGF. Analysis of externally loaded bolted joints: analytical, computational and experimental study. Int J Press Vesssel Pip 2009;86:420–7.
[17] Croccolo D, Agostinise DE, Vincenzi N. Failure analysis of bolted joints: effect of friction coefficients in torque-preloading relationship. Eng Fail Anal 2011;18:364–73.
[18] VDI Handbuch Konstruktion 2230. Systematic calculation of high duty bolted joints – 314 joints with one cylindrical bolt; 2001.
[19] Patterson EA. A comparative study of methods for estimating bolt fatigue limits. Fatigue Fract Mater Struct 1990;13:59–81.
[20] Bickford JH. An introduction to the design and behavior of bolted joints. NY: Marcel Dekker, Inc.; 1990.
[21] Goodman J. Mechanics applied to engineering. London: Longmans; 1899.
[22] Burguete RL, Patterson EA. The effect of mean stress on the fatigue limit of high tensile bolts. Proc Inst Mech Eng 1995;209:257–62.